

Development of adenoviral vectors that transduce Purkinje cells and other cerebellar cell-types in the cerebellum of a humanized mouse model

Emre Kul,¹ Uchechi Okoroafor,^{1,2} Amanda Dougherty,¹ Lauren Palkovic,¹ Hao Li,¹ Paula Valiño-Ramos,¹ Leah Aberman,¹ and Samuel M. Young, Jr.^{1,2,3,4}

¹Department of Anatomy and Cell Biology, University of Iowa, Iowa City, IA 52242, USA; ²Cell Developmental Biology Graduate Program, University of Iowa, Iowa City, IA 52242, USA; ³Department of Otolaryngology, University of Iowa, Iowa City, IA 52242, USA; ⁴Iowa Neuroscience Institute, University of Iowa, Iowa City, IA 52242, USA

Viral vector gene therapy has immense promise for treating central nervous system (CNS) disorders. Although adeno-associated virus vectors (AAVs) have had success, their small packaging capacity limits their utility to treat the root cause of many CNS disorders. Adenoviral vectors (Ad) have tremendous potential for CNS gene therapy approaches. Currently, the most common vectors utilize the Group C Ad5 serotype capsid proteins, which rely on the Coxsackievirus-Adenovirus receptor (CAR) to infect cells. However, these Ad5 vectors are unable to transduce many neuronal cell types that are dysfunctional in many CNS disorders. The human CD46 (hCD46) receptor is widely expressed throughout the human CNS and is the primary attachment receptor for many Ad serotypes. Therefore, to overcome the current limitations of Ad vectors to treat CNS disorders, we created chimeric first generation Ad vectors that utilize the hCD46 receptor. Using a “humanized” hCD46 mouse model, we demonstrate these Ad vectors transduce cerebellar cell types, including Purkinje cells, that are refractory to Ad5 transduction. Since Ad vector transduction properties are dependent on their capsid proteins, these chimeric first generation Ad vectors open new avenues for high-capacity helper-dependent adenovirus (HdAd) gene therapy approaches for cerebellar disorders and multiple neurological disorders.

INTRODUCTION

Due to the clinical successes of viral vector-mediated gene therapy,^{1,2} it is an attractive strategy to treat many CNS disorders. Although adeno-associated virus vectors (AAVs) have many positives, which include the most clinical successes for Food and Drug Administration-approved gene therapies,^{2,3} major drawbacks of both AAV and lentiviral vectors (LVV) are the packaging capacity of ~5 kb and ~9 kb, respectively,^{1,4,5} rendering them incompatible as approaches to treat the root cause of many genetic CNS disorders that are due to mutations in genes that encode large cDNAs.^{6,7,8,9} Therefore, AAV approaches are not viable strategies as the cDNAs simply do not fit within AAV. Furthermore, the relative size of LVVs to their foreign DNA payload will result in significantly low viral titers,^{10,11} which severely limits their utility. Although Herpes-Simplex Virus

Type 1 (HSV-1) amplicon vectors have a large packaging capacity, these vectors suffer from serious safety concerns and are not viable options for use in the clinic.¹²

Adenoviral vectors have tremendous potential for treatment of CNS disorders and are currently being used in human clinical trials.^{13,14} The most commonly used Ad vectors used in the CNS are based on Ad Group C Serotype 5 (Ad5), which transduces cells via Coxsackie-Adenovirus receptor (CAR).¹⁵ However, these Ad5 vectors are unable to transduce many neuronal cell types that are dysfunctional in many CNS disorders. In particular, many hereditary cerebellar disorders are due to Purkinje cell (PC) dysfunction or degeneration.^{7,16,17} Since PCs mediate the only information outflow from cerebellar cortex and due to PC-related pathologies observed in cerebellar disorders, they are the key cell type to target to treat these disorders.¹⁸ However, CAR expression in the mouse and human cerebellum is very low^{19,20} and an extremely small subset of human PCs express CAR.²¹ Furthermore, *in vivo* injections of Ad5 resulted in little to no transduction of PCs,^{22,23} while transduction of mouse dissociated cerebellar cultures showed that only 1.6% of PCs were transduced with an Ad5 vector.²⁴ As a result, for ~25 years^{22–25} the use of Ad vectors in the cerebellum has been abandoned. Therefore, a novel first generation Ad that can transduce PCs and potentially other cerebellar cell types is needed before Ad gene therapy approaches can be developed to treat cerebellar disorders.

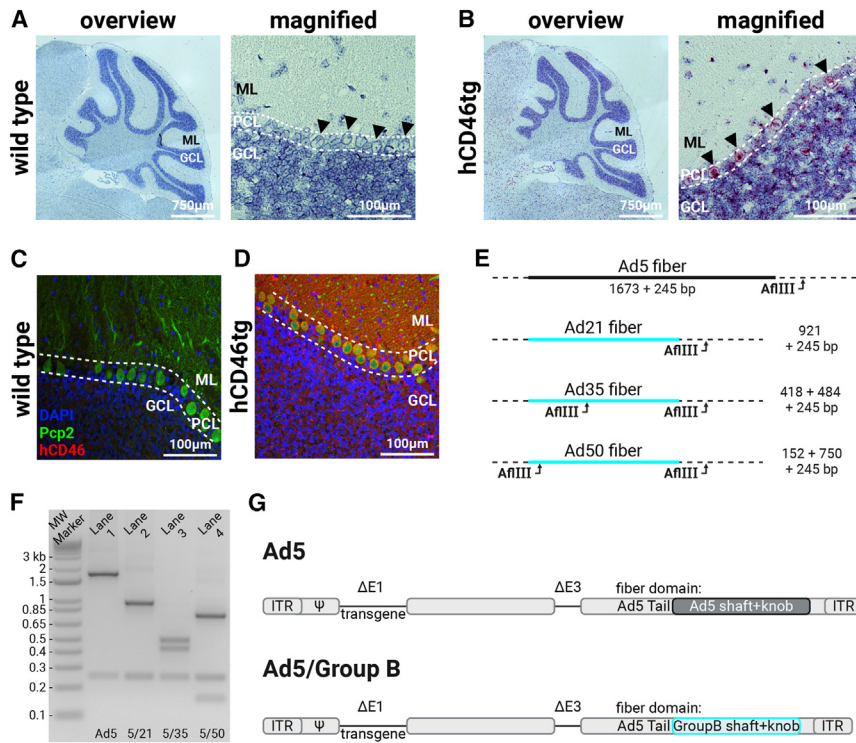
The development of chimeric Ad5 vectors, which contain fibers from other Ad serotypes, is well-established in generating Ad vectors that transduce refractory cell types.^{26,27} Group B Ads use the human CD46 receptor (hCD46),²⁸ which has ubiquitous expression in human cells.^{29,30} Since the Ad capsid proteins are the key determinants of viral vector tropism, we generated first generation Ad5/Group B

Received 5 September 2023; accepted 22 March 2024;
<https://doi.org/10.1016/j.omtm.2024.101243>.

Correspondence: Samuel M. Young, Jr., PhD, Department of Anatomy and Cell Biology, University of Iowa, PBDB 5322, 169 Newton Road, PBDB 5322, Iowa City, IA 52242, USA.

E-mail: samuel-m-young@uiowa.edu





fiber chimeric vectors from serotypes 21, 35, or 50, designated as Ad5/21, Ad5/35, and Ad5/50, respectively. Using a validated preclinical humanized mouse model expressing hCD46 (hCD46tg)³¹ in conjunction with stereotactic delivery to the cerebellum, we found that the three chimeric vectors transduced PCs in a hCD46-dependent manner. We also observed that Ad5/35 and Ad5/50 injection into the deep cerebellar nuclei (DCNs) resulted in widespread retrograde transduction of PCs and that a PC-specific promoter led to increased PC transduction.³² Additionally, we determined that both vectors transduced Bergmann glia, granule cells, and cerebellar afferent mossy fibers independently of hCD46. Taken together, our establishment of these chimeric Ad vectors has the potential to serve as platform technology for development of high-capacity helper-dependent adenoviral (HdAd) vectors as HdAd production relies on the use of the capsid proteins of a first generation helper virus Ad vector. Since HdAd has a large ~36 kb packaging capacity, HdAd vectors with hCD46 dependent tropism have tremendous potential for viral vector gene therapy approaches to treat hereditary cerebellar ataxias and potentially other neurological disorders requiring expression of large transgenes or multiple transgene cassettes.

RESULTS

PCs in the hCD46tg cerebellum express hCD46

hCD46 transgenic mice (hCD46tg) are considered an excellent preclinical model for assessing Ad vectors that utilize hCD46 to transduce cells.^{33–35} Although human PCs express hCD46^{36,37} and measles virus infects similar human CNS cell populations, which include the cerebellum in the hCD46tg mouse,³¹ it was unknown if PCs in

hCD46tg mice express hCD46. Therefore, to determine hCD46 expression in PCs, we performed BaseScope and immunofluorescence (IF) on cerebellar sections from the hCD46tg mice. Our results from the BaseScope assay demonstrated that hCD46 mRNA is expressed throughout the hCD46tg brain and in PCs, while wild-type mice did not express hCD46 (Figures 1A and 1B). Subsequently, we performed IF against hCD46 together with L7/Pcp2, a PC-specific molecular marker, to validate hCD46 expression at the protein level in the hCD46tg mouse cerebellum. We found hCD46 expression by PCs and other cell types in the molecular and granular cell layers of the hCD46tg cerebellum (Figure 1D). Antibody specificity was confirmed via lack of signal in cerebellar sections of wild-type mice (Figure 1C). Since the IF confirmed our BaseScope results, we used hCD46tg mice to investigate hCD46-dependent Ad vector transduction in the cerebellum.

Generation of Group B chimeric adenoviral vectors

The adenovirus fiber, which consists of the shaft and knob region, is a key determinant of vector tropism.^{26,38} Group B Ads use hCD46 as their primary attachment receptor.²⁸ Since Ad5 chimeras, which contain fibers from other Ad serotypes, can transduce cells refractory to Ad5, and can be produced to high titers,^{26,27} we developed first generation E1, E3-deleted Ad5/Group B fiber “chimeric vectors.” To do so, we replaced the Ad5 fiber with the Group B Serotype 50, or 35, or 21 fiber (Figure 1G). Ad50 and Ad21 are in the same fiber knob clade with protein sequences differing by a single amino acid, while Ad35 is in a distinct fiber knob clade. In addition, Ad21 and A50 are Group B1, while Ad35 is a Group B2 virus. Furthermore

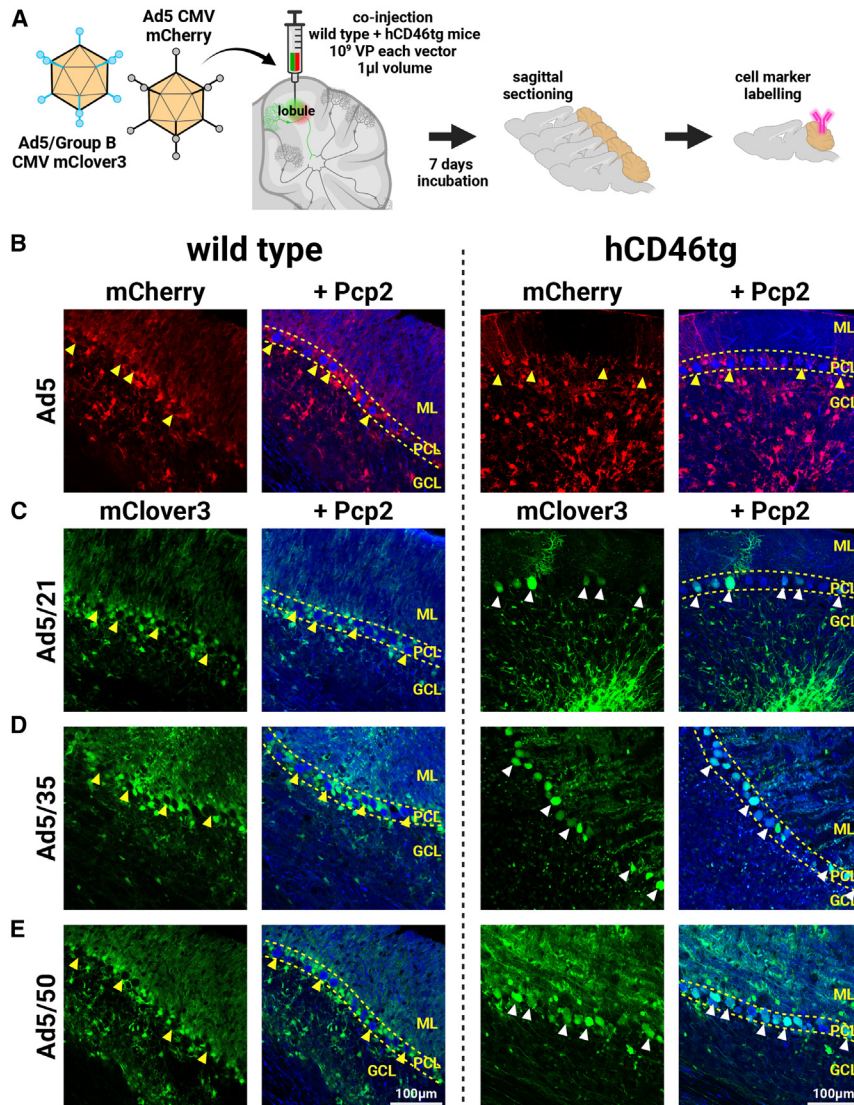


Figure 2. hCD46-dependent transduction of Purkinje cells by Group B chimeric vectors

(A) Illustration showcasing lobular administration of Ad5 individually co-mixed with Ad5/21, Ad5/35, or Ad5/50 into the mouse cerebellum and subsequent tissue processing steps. N(wt/tg) = 3/3 for each chimeric vector. VP, viral particle. (B) Fluorescent photomicrographs representing lack of Ad5 tropism to PCs in the cerebellar cortex of wild-type (left column) and hCD46tg (right column) mice. Red: Ad5 transduction signal (mCherry), Blue: Pcp2 immunofluorescence signal. ML, molecular layer; PCL, Purkinje cell layer; GCL, granule cell layer. Yellow arrowheads indicate non-transduced PCs, dashed lines indicate PCL. (C–E) Fluorescent photomicrographs representing Ad5/21 (C), Ad5/35 (D), and Ad5/50 (E) tropism to PCs in the cerebellar cortex of wild-type (left column) and hCD46tg (right column) mice. Green: chimeric vector transduction signal (mClover3). White arrowheads indicate transduced PCs. Data are derived from co-injections of each Ad5/Group B vector with the Ad5 vector, where 1×10^9 VP per vector was delivered in 1 μ L volume into the cerebellar simple lobule.

mice. Viral particle numbers were used since these were qualitative experiments to determine if the chimeric vectors could transduce PCs or not. Subsequently, 7 days later, we euthanized the animals, generated cerebellar sections, and used immunofluorescent labeling against the PC-specific marker, L7/Pcp2, to analyze co-localization of mClover3 and the PCs (Figure 2A). We found that Ad5 transduction (mCherry signal) in the cerebellar cortex did not overlap with L7/Pcp2 in wild-type or in hCD46tg tissue (Figure 2B). In contrast, we detected mClover3 within cells that were positive for L7/Pcp2 in hCD46tg cerebellar tissue from mice injected with either Ad5/21 (Figure 2C, right column), or Ad5/35 (Figure 2D, right column), or Ad5/50 (Figure 2E, right column). However, we did not find any overlap of mClover3 and L7/Pcp2 signal in the wild-type mice with Ad5/21 (Figure 2C, left column), or Ad5/35 (Figure 2D, left column), or Ad5/50 (Figure 2E, left column). Based on these results, we conclude that Ad5-derived Group B chimeric vectors can transduce PCs in the hCD46tg mouse and transduction is hCD46-dependent.

Injections of Ad5/35 and Ad5/50 in the deep cerebellar nuclei result in PC transduction

Ad5 vectors are capable of transducing neurons through retrograde axonal transport.^{22,39–42} Since the DCN are the convergence point of all PC axonal terminals,⁷ the ability to transduce PCs through retrograde transport has the potential to induce widespread PC transduction as an alternative to multiple injections into many cerebellar lobules. Ad5 vectors can transduce PCs at extremely low levels through injection into the DCN.^{22,23} Therefore, to investigate if our

Ad5/35 chimeric vectors efficiently transduce hCD46tg mouse hematopoietic stem cells.^{33–35} After successful cloning of Ad5/21, Ad5/35, and Ad5/50 genomic plasmids, these chimeric vectors were produced to high titers using standard protocols for first generation Ad production (See materials and methods). Afterward, the chimeric vector identities were confirmed with restriction digestion of PCR fragments of fiber regions amplified from isolated viral DNA from purified stocks (Figures 1E and 1F).

Ad5/21, Ad5/35, and Ad5/50 Group B chimeras transduce PCs

To investigate if the chimeric vectors transduced PCs, we performed stereotactic injections into the cerebellar cortex of the hCD46tg mouse and wild-type controls. To do so, Ad5/50, or Ad5/35, or Ad5/21 (CMV mClover3) were individually co-mixed with equal viral particles of Ad5 (CMV mCherry) and were stereotactically injected into the PC somatic cell layer in the cerebellar simple lobule of adult

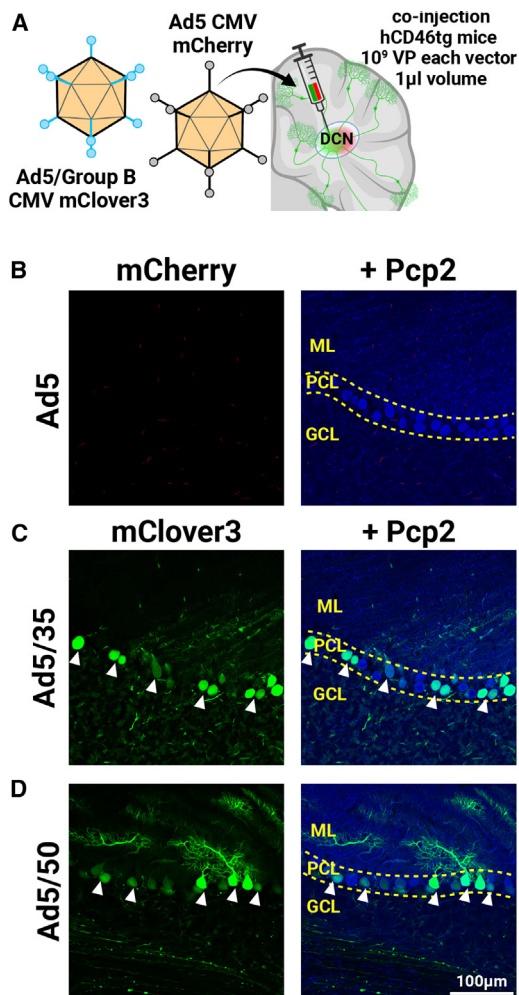


Figure 3. Injection of chimeric vectors into the DCN transduces Purkinje cells via retrograde axonal transport

(A) Illustration of sagittal mouse cerebellum section depicting DCN injection site targeting PC axon terminals. $N(\text{tg}) = 3$ for each chimeric vector. (B) Fluorescent photomicrographs representing lack of Ad5 tropism to PCs in the cerebellar cortex of hCD46tg mice upon DCN injection. Red: Ad5 transduction signal (mCherry), Blue: Pcp2 immunofluorescence signal. ML, molecular layer; PCL, Purkinje cell layer; GCL, granule cell layer. Dashed lines indicate PCL. (C and D) Fluorescent photomicrographs representing transduction of PCs by Ad5/35 (C) and Ad5/50 (D) in the cerebellar cortex of hCD46tg mice upon DCN injection. Green: chimeric vector transduction signal (mClover3). White arrowheads indicate transduced PCs. Data are derived from co-injections of each Ad5/Group B vector with the Ad5 vector, where 1×10^9 VP per vector was delivered in 1 μL volume into the DCN.

chimeric vectors were capable of high levels of retrograde transduction of PCs, we injected these vectors into the DCN of hCD46tg mice (Figure 3A) using a similar approach to our cerebellar lobule injections. For these experiments we focused on Ad5/35 and Ad5/50, since Ad50 and Ad21 are in the same fiber knob clade with protein sequences differing by a single amino acid, while Ad35 is in a distinct fiber knob clade. In addition, Ad21 and A50 are Group B1, while Ad35 is a Group B2 virus. We observed absence of mCherry signal

in the cerebellar cortex indicating that Ad5 was unable to transduce PCs via retrograde transduction (Figure 3B). However, we found that mClover3 expression co-localized with L7/Pcp2 signal in cerebellar sections of animals injected with either Ad5/35 (Figure 3C) or Ad5/50 (Figure 3D). Based on the lack of Ad5 transduction in the cerebellar cortex and the absence of transduction by the chimeric vectors in cell types other than PCs, we conclude that Ad5/35 and Ad5/50 are capable of transducing PCs through retrograde axonal transport.

Since wild-type Ad50 may have higher affinity for hCD46 than wild-type Ad35, we wanted to determine if potential difference in affinities for the hCD46 receptor between Ad5/35 and Ad5/50 impacted retrograde transduction efficiency. To do so, we created an Ad5/50 CMV mScarlet chimeric vector and co-mixed equal transducing units (TUs) of both Ad5/50 CMV mScarlet and Ad5/35 CMV mClover3 vectors and injected into the DCN of hCD46tg mice. Equal TUs of each chimeric vector were used since we wanted to directly compare the Ad5/35 and Ad5/50 efficiencies to transduce PCs. We then quantified the number of PCs transduced by each vector from serially cut cerebellar sections (Figure 4A). We found that there was no significant difference in the total number of PCs transduced between the two vectors (Figure 4B). However, we found that only 28.84% (1.579%) of PCs were positive for both mClover3 and mScarlet fluorescence (Figure 4C). Furthermore, DCN injections of both vectors resulted in widespread PC transduction from the most lateral to the most medial sagittal serial section (Figure 4D). Therefore, our data indicate that a single DCN injection was sufficient to transduce PCs distant to the injection site. Finally, we conclude that neither vector is superior in transducing PCs through DCN injection in the hCD46tg tissue.

The PC-specific promoter improves PC transduction efficiency

Promoters are critical factors that define transduction properties as they impact transgene expression specificity and expression levels. While the CMV promoter leads to ubiquitous high-level expression from viral vectors, use of cell-type-specific promoters has been demonstrated to lead to increased transduction of specific cell types.^{43,44} The L7-6 promoter, which is a derivative of the L7 promoter, is a minimal promoter with high specificity to PCs in the cerebellum.³² Therefore, to determine if we could increase PC transduction with the L7-6 promoter, we created an Ad5/50 L7-6 mScarlet vector. Subsequently, we compared its transduction efficiency to Ad5/50 CMV mClover3 via DCN co-injections that delivered equal TU of each vector. Since the L7-6 promoter is weaker than the CMV promoter, we euthanized the mice 28 days after injection to ensure gene expression from both promoters (Figure 5A). By quantifying the number of PCs transduced by each vector from serial cerebellar sections, we found that Ad5/50 L7-6 mScarlet led to significantly higher number of PCs transduced compared with Ad5/50 CMV mClover3 (820.3 (73.10) vs. 559.7 (24.17), $p = 0.0173$, t test) (Figure 5B). Although, both vectors transduced PCs in the cerebellar cortex, we observed that only 22.36% (5.821%) of PCs were co-transduced by the two vectors (Figure 5C). Further analysis revealed that

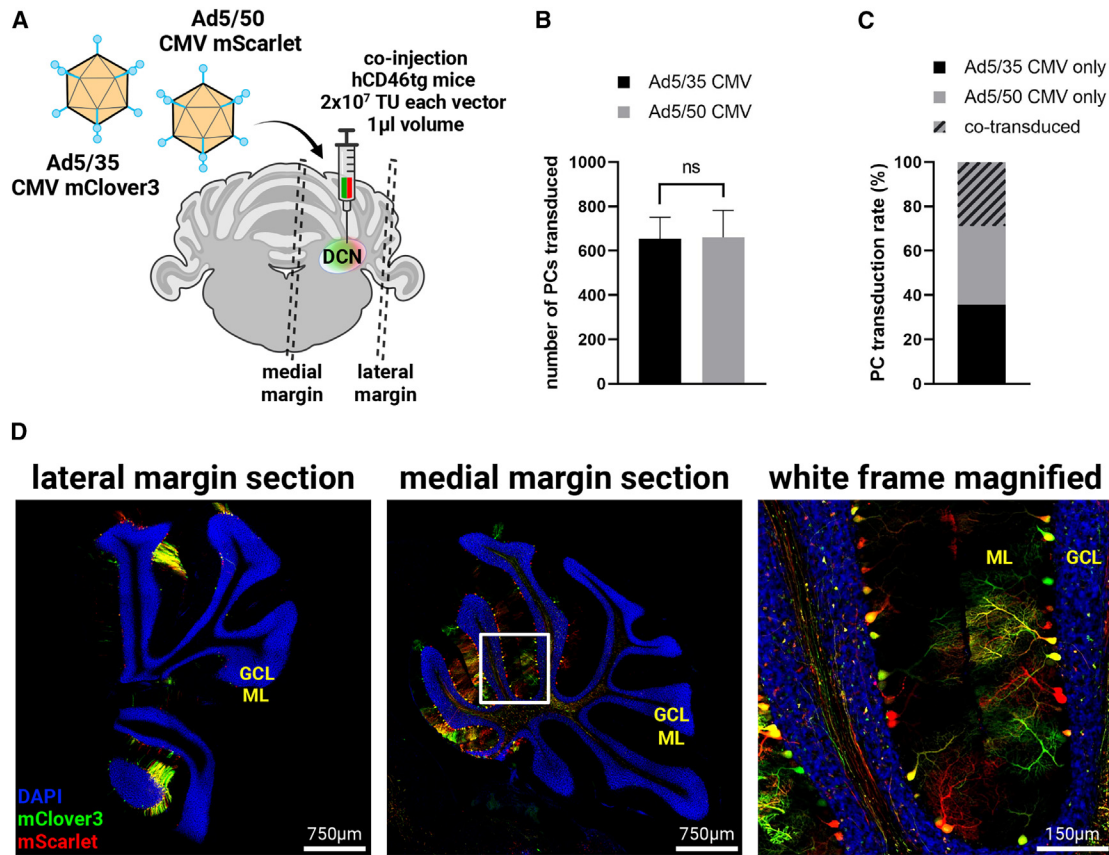


Figure 4. Ad5/35 and Ad5/50 transduce comparable number of Purkinje cells via DCN

(A) Illustration of coronal mouse cerebellum section depicting DCN injection performed to compare Ad5/35 with Ad5/50 and margin sections obtained distant to the injection site (dashed lines). $N(\text{tg}) = 3$. TU, transducing units. (B) Quantification from sagittal serial sections of number of PCs transduced by either Ad5/35 or Ad5/50 under CMV promoter. ns, $p = 0.9678$, Student's *t* test. Data are plotted as mean \pm SEM. (C) Stacked bar graph indicating the percentage of PCs transduced by each vector and the percentage co-transduced by both vectors. (D) Tiled photomicrographs representing PC transduction at the lateral margin (left) and medial margin (middle) of the cerebellum. Magnified reproduction (right) of the white frame on the medial margin section. Green: Ad5/35 vector transduction signal (mClover3), Red: Ad5/50 vector transduction signal (mScarlet), Blue: DAPI, ML: molecular layer, GCL: granule cell layer. Data are derived from co-injections of the Ad5/35 vector with the Ad5/50 vector, where 2×10^7 TU per vector was delivered in 1 μL volume in to the DCN.

the transduction patterns of the two vectors differed significantly from each other. At the DCN injection site, numerous cell bodies were labeled by Ad5/50 CMV vector, while we rarely observed any signal from the Ad5/50 L7-6 vector that is consistent in size and shape with transduced cell somata (Figure 5D). Based on these data, we conclude that L7-6 promoter results in higher PC transduction efficiency and as reported previously,³² restricts the transgene expression to PCs.

Ad5/35, Ad5/50: hCD46-independent tropism in the cerebellar cortex

Despite their ability to bind hCD46, Group B Ads can utilize a variety of other cell surface receptors for transduction.⁴⁵ Our results from lobular injections in the wild-type mice showed that Group B chimeras did not transduce PCs (Figures 2C–2E); however, we observed viral transduction in other cell types. Therefore, we characterized transduction of Ad5/35 CMV mClover3 and Ad5/50 CMV

mClover3 using immunofluorescence against cell-type-specific molecular markers. We co-injected these vectors with Ad5 CMV mCherry with equal viral particles for each vector into the cerebellar simple lobule as these were qualitative experiments (Figures 6, 7, and 8). Previously, it has been reported that Ad5 vectors can efficiently transduce Bergmann glia.²⁴ Therefore, to examine if the Ad5/35 and Ad5/50 vectors transduced Bergmann glia, we used s100 β as a non-specific glial marker and identified Bergmann glia based on their location and morphology. All vectors including Ad5, transduced Bergmann glia both in the wild-type and hCD46tg mice (Figures 6A–6C). Since Ad5 vectors can transduce granule cells *in vitro* and in organotypic cultures,²⁴ we next examined granule cell transduction. To do so, we used NeuN as a marker of granule cells in the cerebellar cortex. We found that Ad5/35 and Ad5/50 vectors transduced low numbers of granule cells in a scattered pattern (Figures 7B and 7C) both in the wild-type and in the hCD46tg tissue, but Ad5 signal did not co-localize with NeuN

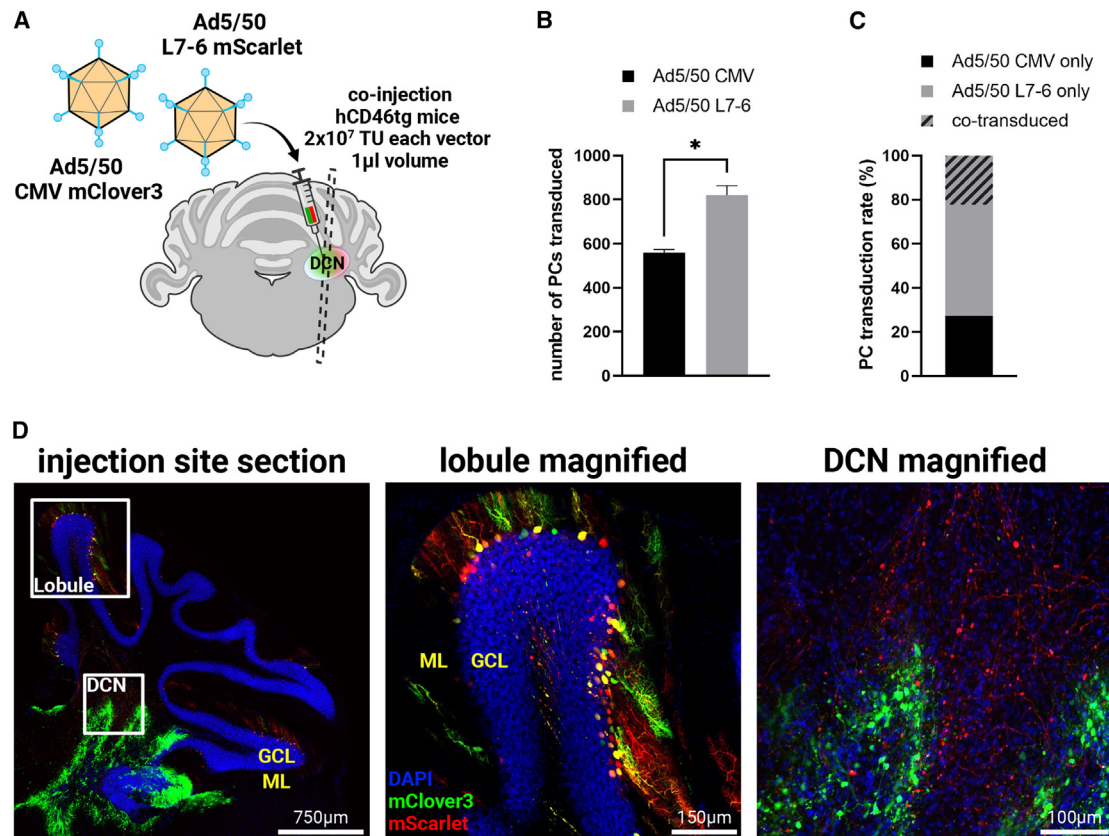


Figure 5. PC-specific L7-6 promoter increases transduction efficiency

(A) Illustration of coronal mouse cerebellum section depicting DCN injection performed to compare CMV promoter to L7-6 promoter under the context of Ad5/50. $N(tg) = 3$. Dashed lines indicate section obtained from proximity to the injection site. TU: transducing units. (B) Quantification of number of PCs from sagittal serial sections transduced by Ad5/50 under either CMV or L7-6 promoters. *, $p = 0.0173$, Student's t test. Data are plotted as mean \pm SEM. (C) Stacked bar graph indicating the percentage of PCs transduced by each vector and the percentage co-transduced by both vectors. (D) Tiled photomicrograph representing Ad5/50 tropism at the injection site section (left) and magnified images corresponding to the lobule frame (middle) and DCN frame (right). Green: Ad5/50 CMV vector transduction signal (mClover3), Red: Ad5/50 L7-6 vector transduction signal (mScarlet), Blue: DAPI, ML, molecular layer; GCL, granule cell layer; DCN, deep cerebellar nuclei. Data are derived from co-injections of the Ad5/50 CMV vector with the Ad5/50 L7-6 vector, where 2×10^7 TU per vector was delivered in $1 \mu\text{L}$ volume into the DCN.

signal (Figure 7A). Finally, since Ad5 vectors and our Group B chimeras are capable of retrograde transduction, we examined afferent mossy fibers that make glutamatergic synapses in the granule cell layer of multiple cerebellar lobules. We observed cell bodies transduced by the Group B chimeras in various nuclei such as the ECU: external cuneate nucleus, RN: reticular nuclei, PRN: pontine reticular nucleus in the pons and medulla, which are part of several brainstem nuclei, where mossy fibers originate from^{46,47} (Figure 8A left). Consistent with their axonal topology,^{46,47} we detected mClover3-labeled mossy fibers in the injected simple lobule (Figure 8A solid frame - middle) and in various non-injected lobules (Figure 8A dashed frame - right). Since the transduction signal from mossy fiber terminals are partly masked by somatic transduction at the injected lobule, we further examined non-injected lobules using vGlut1 immunostaining. Although we did not detect mCherry signal in mossy fiber terminals, which indicated lack of Ad5 transduction (Figure 8B), we observed both Ad5/35 and Ad5/50 driven

mClover3 signal co-localized with vGlut1 in the wild-type and in the hCD46tg tissue (Figures 8C and 8D). Taken together, we conclude that chimeric vectors can transduce various cell types independent of the hCD46 expression and exhibit distinct tropism from Ad5.

DISCUSSION

In this study, we demonstrated that Ad5/Group B fiber chimeras, Ad5/50, Ad5/35, and Ad5/21 efficiently transduce PCs *in vivo* in a humanized hCD46 transgenic (hCD46tg) mouse model. In addition, we found Ad5/35 and Ad5/50 were capable of efficient PC transduction through retrograde transport and were able to transduce other cell types in the cerebellum. Since hCD46 is ubiquitously expressed in human cells, these chimeric viral vectors can be used as platform technology for the development of HdAd gene therapy approaches not only for hereditary cerebellar ataxias but also for other human neurological disorders.

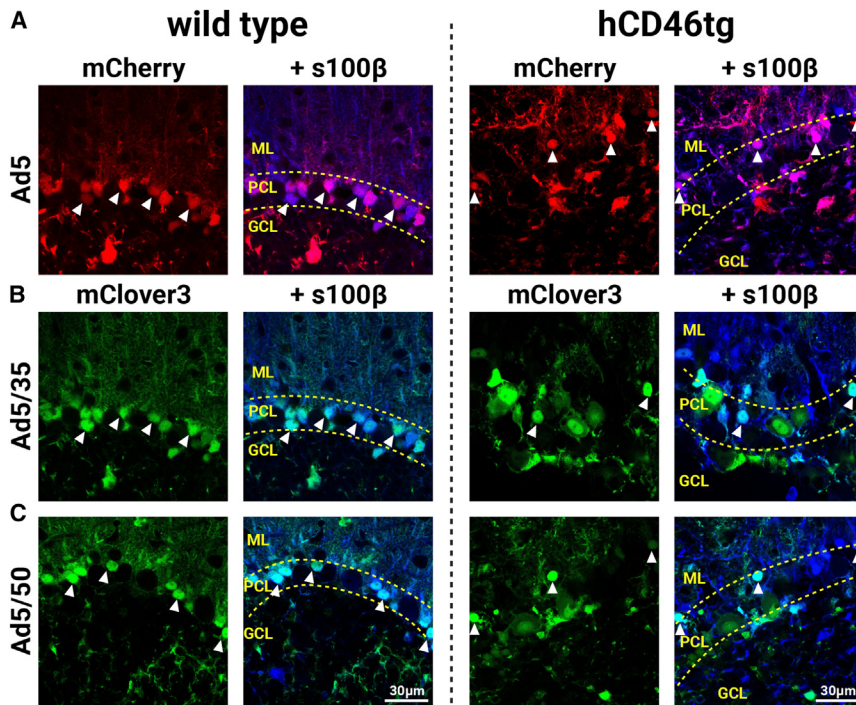


Figure 6. Ad5, Ad5/35, and Ad5/50 transduce Bergmann glia in a hCD46 independent manner

(A) Fluorescent photomicrographs representing Ad5 tropism to Bergmann glia in wild-type (left column) and hCD46tg (right column) mice. Red: Ad5 transduction signal (mCherry), Blue: s100 β immunofluorescence signal. ML, molecular layer; PCL, Purkinje cell layer; GCL, granule cell layer. (B and C) Fluorescent photomicrographs representing Ad5/35 (B) and Ad5/50 (C) tropism to Bergmann glia in wild-type (left column) and hCD46tg (right column) mice. White arrowheads indicate transduced Bergmann glia. Green: chimeric vector transduction signal (mClover3). N(wt/tg) = 3/3 for each chimeric vector. Data are derived from co-injections of each Ad5/Group B vector with the Ad5 vector, where 1×10^9 VP per vector was delivered in 1 μ L volume into the cerebellar simple lobule.

The hCD46tg model

Our studies relied on the established hCD46tg mouse, which exhibits hCD46 expression patterns and levels that mimic expression patterns observed in humans.³¹ More importantly, hCD46 expression in this mouse line renders them susceptible to measles infections and infects similar human CNS cell populations, which include the cerebellum.³¹ Our immunofluorescence characterization showed that hCD46tg mouse PCs express hCD46, which is similar to human PCs.^{36,37} Since every human enucleated cell expresses hCD46,^{29,30} the ability of the Ad5/Group B fiber chimeras to transduce PCs in hCD46tg mice indicate that these vectors will have tremendous clinical potential. Prior work has demonstrated that the Ad5/35 and HdAd5/35 vectors successfully transduce hematopoietic stem cell populations from hCD46tg mice and non-human primates.^{33–35,48} Furthermore, intravenous administration of HdAd5/35 vectors in hCD46tg mice and non-human primates led to similar biodistribution between the two animals.⁴⁹ Therefore, this mouse model provides a valuable framework for evaluating the efficacy and development of Ad5/Group B fiber chimeric vectors or Group B Ad vectors in transducing other neuronal cell types that are refractory to Ad5 transduction in the CNS in general. More importantly, the hCD46tg mouse can be used in conjunction with other neurological disorder mouse models as preclinical platforms for the development of gene therapy approaches that utilize HdAd5/Group B fiber chimeras or HdAd Group B vectors.

Ad5/21, Ad5/35, and Ad5/50 transduce PCs in the hCD46tg mouse model

Our finding that the Ad5/21, Ad5/35, and Ad5/50 transduce PCs in the hCD46tg mice but not in wild-type mice indicates that hCD46

expression is sufficient for PC transduction. However, we did not find differences in the efficiency of different chimeras in transducing PCs. Therefore, our data indicate that potential differences between Ad21, Ad35, and Ad50 fiber binding affinities to hCD46 are not key determinants in PC transduction. Although hCD46 is

expressed on every enucleated cell, Ad21, Ad35, and Ad50 have distinct cell-type tropism.⁴⁵ Although differences in Group B fiber affinity for hCD46 is proposed to underpin the distinct tropisms,⁵⁰ there is no consensus if the fiber binding affinity is a key determinant of cell-type transduction. Based on *in vitro* hCD46 binding assays, the Ad35 fiber is considered to have high affinity to hCD46, while Ad21 fiber displays low affinity.⁵⁰ In contrast, assays examining the attachment of Group B Ads to hCD46 expressing cell lines showed that the number of Ad50 and Ad21 viruses attached to the hCD46 expressing cells is significantly higher than Ad35.²⁸ Furthermore, in cell lines, Ad viral vectors with engineered Ad35 fibers with higher affinity for hCD46 did not lead to increased transduction efficiencies compared with the native Ad35 fiber.⁵¹ However, it is speculated that other steps that contribute to transduction are impacted by the difference in fiber binding affinity leading to higher transduction in certain tissues.⁵¹

Retrograde transduction of PCs with Ad5/35 and Ad5/50

The cerebellum has multiple lobules, which creates a complicated architecture in which to target maximal transduction coverage of all PCs. Thus, although targeting PCs through multiple lobular injections would be feasible, an alternative delivery approach would be ideal. Since all PCs input into the DCN, the ability to utilize retrograde transport to transduce PCs is an attractive strategy. Ad5 vectors are capable of transducing neurons via retrograde transduction with canine adenoviral vectors being one of the most efficient.⁵² Adenovirus fibers are involved in intracellular trafficking and uncoating kinetics,⁵¹ which may influence retrograde transduction efficiency. While Ad5 vectors are

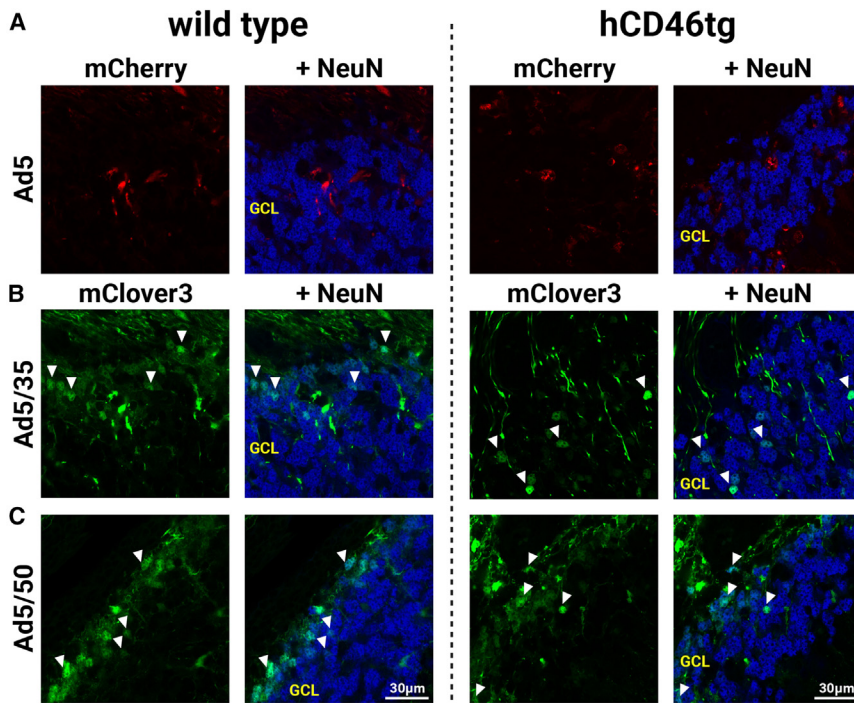


Figure 7. Ad5/35 and Ad5/50 transduce granule cells in a hCD46 independent manner

(A) Fluorescent photomicrographs of granule cell layer representing lack of Ad5 tropism to granule cells in wild-type (left column) and hCD46tg (right column) mice. Red: Ad5 transduction signal (mCherry), Blue: NeuN immunofluorescence signal. GCL, granule cell layer. (B and C) Fluorescent photomicrographs of granule cell layer representing Ad5/35 (B) and Ad5/50 (C) tropism to granule cells in wild-type (left column) and hCD46tg (right column) mice. White arrowheads indicate transduced granule cells. Green: chimeric vector transduction signal (mClover3). N(wt/tg) = 3/3 for each chimeric vector. Data are derived from co-injections of each Ad5/Group B vector with the Ad5 vector, where 1×10^9 VP per vector was delivered in 1 μ L volume into the cerebellar simple lobule.

localization.^{51,54} Finally, it will be important to compare the retrograde transduction between Canine Ads and the Ad5/Group B fiber chimeric vectors.

capable of retrograde transduction and can transduce PCs through retrograde transduction via DCN injection, it is extremely inefficient.^{22,23}

We found that injection of Ad5/35 and Ad5/50 into the DCN led to highly efficient transduction of PCs with broader transduction areas compared with the injection into the lobule. Furthermore, our data showed that Ad5 injection into the DCN did not lead to PC transduction in both mouse genotypes, but DCN injection of Ad5/35 and Ad5/50 in the wild-type mice did not lead to PC transduction. Therefore, our data indicate that Ad35 and Ad50 fibers are responsible for retrograde transduction and that PC presynaptic terminals contain hCD46 receptors. Since Ad fibers target Ad virions to distinct trafficking pathways, it is likely that the Ad35 and Ad50 fibers target the chimeric vectors to trafficking pathways that lead to retrograde transduction. Based on previous work, the Ad35 fiber targets Ad5/35 chimeras to the late endosomal and lysosomal compartments and it is postulated that this leads to proximity to the nucleus.^{51,53} Since both Ad5/50 and Ad5/35 led to similar levels of retrograde transduction, this suggests that both Ad50 and the Ad35 fiber target the chimeras to the same trafficking pathways. However, future studies need to be carried out to determine the trafficking of these vectors in PCs and neurons in general. Additionally, we found that only ~29% of all transduced PCs were co-transduced by both Ad5/35 and Ad5/50 via DCN injection. While this may be due to distinct trafficking pathways, it is possible that the competition between the viral vectors for the hCD46 receptor and potential downregulation of hCD46 after binding is the mechanism behind partial co-

transduction. Since the Ad5/35 and Ad5/50 vectors transduced PCs over a broad area via injection into the DCN, this suggests that DCN injection could be a clinically translatable approach for HdAd-based cerebellar gene therapy. Although intraparenchymal injections are an invasive approach, this is currently utilized in numerous AAV clinical and preclinical trials and other clinical trials for viral vector delivery to the human brain^{55–58} as gene therapy approaches for neurological disorders such as Huntington’s disease ([ClinicalTrials.gov: NCT04120493](https://clinicaltrials.gov/ct2/show/study/NCT04120493), [NCT05243017](https://clinicaltrials.gov/ct2/show/study/NCT05243017)), Parkinson’s disease ([ClinicalTrials.gov: NCT01621581](https://clinicaltrials.gov/ct2/show/study/NCT01621581), [NCT04167540](https://clinicaltrials.gov/ct2/show/study/NCT04167540), [NCT00195143](https://clinicaltrials.gov/ct2/show/study/NCT00195143), [NCT00643890](https://clinicaltrials.gov/ct2/show/study/NCT00643890), [NCT05603312](https://clinicaltrials.gov/ct2/show/study/NCT05603312), [NCT00229736](https://clinicaltrials.gov/ct2/show/study/NCT00229736)), multiple system atrophy ([ClinicalTrials.gov: NCT04680065](https://clinicaltrials.gov/ct2/show/study/NCT04680065)), Alzheimer’s disease ([ClinicalTrials.gov: NCT05040217](https://clinicaltrials.gov/ct2/show/study/NCT05040217)), Batten disease ([ClinicalTrials.gov: NCT01161576](https://clinicaltrials.gov/ct2/show/study/NCT01161576)), and Tay-Sachs disease ([ClinicalTrials.gov: NCT04669535](https://clinicaltrials.gov/ct2/show/study/NCT04669535)). Although the DCN is a deep tissue area, magnetic resonance imaging-guided delivery has significantly improved precision and minimized tissue damage, successfully delivering AAV vectors to deep brain areas such as the substantia nigra pars compacta and ventral tegmental area.⁵⁷ While currently it is not known the level of PC transduction needed to halt cerebellar disease progression, it is likely that large numbers of PCs throughout the cerebellum will be needed. Convection-enhanced delivery (CED) of viral vectors through intraparenchymal injection has been optimized to transduce large areas of the brain.⁵⁹ More importantly, CED has been safely used to treat aromatic-L-amino acid decarboxylase deficiency (AADC) with an AAV2-AADC gene therapy approach in children.⁵⁵ Therefore, exploring CED of the Ad5/Group B chimeras to the DCN has great potential to maximize PC transduction needed to attain therapeutic effects. Future experiments will be needed.

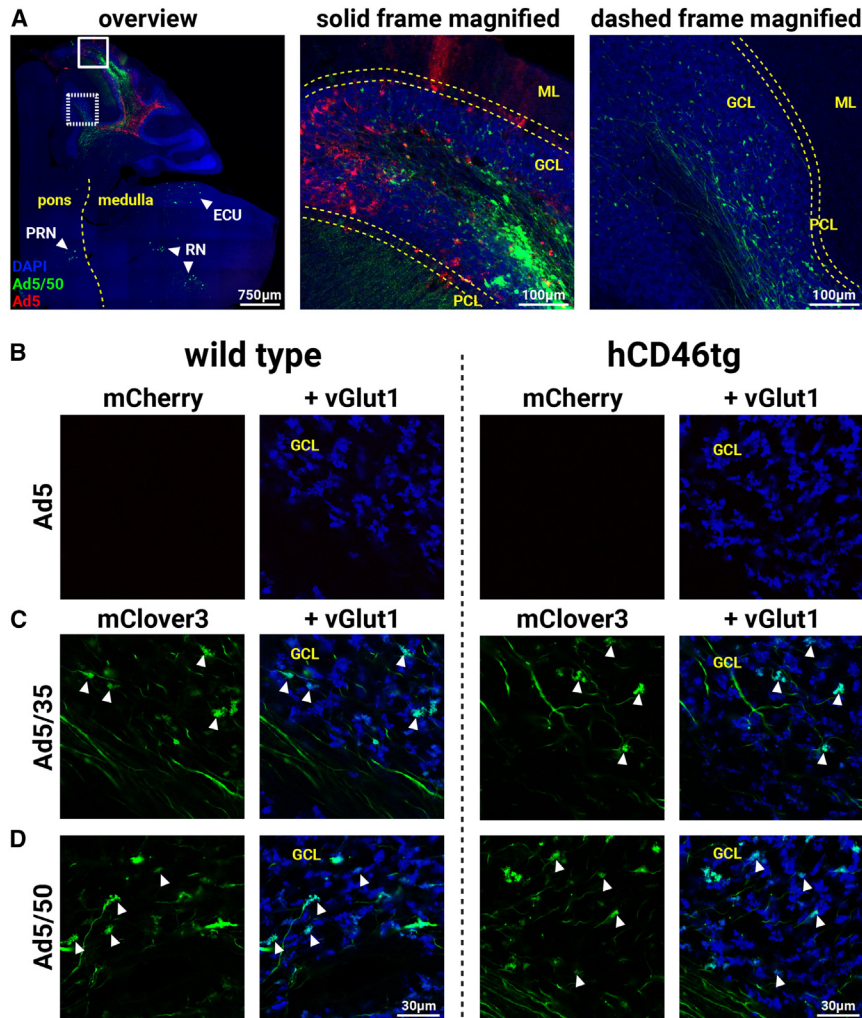


Figure 8. Ad5/35 and Ad5/50 transduce mossy fibers in a hCD46 independent manner

(A) Tiled photomicrograph indicating retrograde transduction of mossy fibers leading to labeling of cell somata in various nuclei in pons and medulla. ECU, external cuneate nucleus; RN, reticular nuclei; PRN, pontine reticular nucleus. Dashed line traces the pontomedullary junction (left). Magnified image corresponding to the solid frame (middle) shows the transduction patterns at the injected simple lobule. Dashed frame indicates transduced mossy fiber terminals by Ad5/50 (green-mClover3) but not by Ad5 (red-mCherry) in a cerebellar lobule distant to the injected lobule (right). ML, molecular layer; PCL, Purkinje cell layer; GCL, granule cell layer. Blue: DAPI. Dashed lines in magnified reproductions indicate PCL. Representative image originates from a hCD46tg mouse. (B) Fluorescent photomicrographs of granule cell layer representing lack of Ad5 transduction of mossy fiber terminals in wild-type (left) and hCD46tg (right) mice. Red: Ad5 transduction signal (mCherry), Blue: vGlut1 immunofluorescence signal. (C and D) Fluorescent photomicrographs of granule cell layer representing Ad5/35 (C) and Ad5/50 (D) transduction of mossy fiber terminals in wild-type (left) and hCD46tg (right) mice. White arrowheads indicate transduced mossy fiber terminals. Green: chimeric vector transduction signal (mClover3). N(wt/tg) = 3/3 for each chimeric vector. Data are derived from co-injections of each Ad5/Group B vector with the Ad5 vector, where 1×10^9 VP per vector was delivered in $1 \mu\text{L}$ volume into the cerebellar simple lobule.

approaches. In addition, CaMKII α or neuron-specific synapsin promoters were found to slightly improve PC transduction efficiencies compared with the ubiquitous CAG promoter.⁶¹ However, further investigations are needed to directly compare the L7-6 with L7-4 or

CaMKII α , or synapsin promoters to determine the most suitable promoter for HdAd-based cerebellar gene therapy.

Ad5/35 and Ad5/50 transduce multiple cell types in the cerebellum

While our study was largely focused on the ability of our chimeric vectors to transduce PCs, we found that the chimeric vectors led to transduction of Bergmann glia, mossy fibers, and granule cells. Interestingly, we found that transduction was not dependent on hCD46 as similar transduction patterns with Ad5/35 and Ad5/50 were seen in both the hCD46tg and wild-type mouse. However, transduction of granule cells and mossy fibers was dependent on the fiber of Ad35 and Ad50, as this transduction pattern was not seen with Ad5. In contrast, Ad5/35, Ad5/50, and Ad5 transduced Bergmann glia. In the absence of fiber-mediated interaction, adenoviruses can utilize direct interaction between the penton base and cell surface integrins for attachment.⁶² Since all the chimeras utilize the Ad5 penton, this interaction could mediate uptake of the viral particles into the cells. Subsequently, once inside the cell the Ad35 and Ad50 fibers could

The L7 promoter leads to increased PC transduction efficiency

Our study utilized the CMV promoter to evaluate PC transduction efficiency. While the CMV promoter is a strong ubiquitous promoter, promoters that drive strong ubiquitous expression can lead to toxicity due to overexpression of the gene of choice or undergo gene silencing.^{2,60} Therefore, the use of more endogenous cell promoters is ideal. The L7-6 promoter is the smallest version of the L7 promoter that confers PC specificity, which in the context of AAV and LVV drives high levels of expression in PCs.³² The L7-6 promoter is more restrictive to PCs compared with the smaller L7-4 version of the promoter.³² Our data showed that similar to AAV and LVV, the L7-6 promoter leads to an increase in specificity of expression compared with the CMV promoter. Although the L7-6 version leads to high PC specificity, it may not be an ideal promoter to utilize for treating monogenic cerebellar disorders as the mutant genes underlying these disorders are expressed in a wide variety of cell types that may also contribute to the disease phenotype. Thus, L7-4 promoter, which leads to expression in multiple cerebellar cell types in addition to PCs may be ideal to be utilized in the context of HdAd gene therapy

target the viral particles to a different trafficking pathway than Ad5,⁴² which leads to differences in transduction. In support of this hypothesis, we found that mossy fibers were transduced. Mossy fibers are long-range afferent fibers that originate from multiple nuclei outside of the cerebellum synapsing on multiple cerebellar lobules.^{22,23} Thus, the only way for mossy fibers to be mClover3 positive including in the non-injected lobules would be via retrograde transduction of their cell bodies distant to the injection site. Although the Ad35 and Ad50 fibers are considered to be hCD46 exclusive,⁴⁵ it is possible that these fibers can interact with an alternative receptor distinct from hCD46 or CAR.

Implication for HdAd gene therapy approaches for cerebellar and neurological disorders

Taken together, our work has identified that Group B Ad fibers are sufficient to transduce PCs and other cell types in the hCD46tg mouse model. HdAd production relies on a first generation Ad helper virus and the capsid proteins of the first generation helper virus are the key determinant of viral vector transduction. Therefore, these first generation Ad chimeric vectors can be quickly developed into helper viruses for HdAd production to develop HdAd Group B chimeric vectors. More importantly, the use of Ad5/Group B chimeric vectors opens up new avenues for Ad and HdAd gene therapy applications, not only for cerebellar disorders but also for multiple neurological disorders that cannot be addressed by AAV and LVV. Future studies will be needed to characterize vector tropism in non-human primates and to investigate engineering of Ad capsids and surgical delivery methods maximizing Ad vector spread in the brain.

MATERIALS AND METHODS

Animals

Human CD46 transgenic mice (hCD46tg also known as MYII) on C57/Bl6J background were purchased from the Jackson Laboratory, Bar Harbor, ME (B6.FVB-Tg(CD46)2Gsv/J, RRID:IMSR_JAX:004971) and housed at the University of Iowa Office of Animal Resources facilities under standard laboratory conditions. These mice carry the YAC-CD46 transgene containing full-length human CD46 gene expressed under its endogenous promoter.³¹ The mice were bred under a scheme to produce offspring that are either wild type or heterozygous for the transgene. Littermates aged from P30 to P60 of both genotypes and sexes were used for the study. The genotyping was done to the tissue obtained from earmark clippings using a standard PCR protocol described by the Jackson Laboratory. All animal procedures were approved by the University of Iowa Institutional Animal Care and Use Committee (Protocol # 0122358).

Viral vectors

E1, E3-deleted first generation adenoviral vectors were created under the 2-plasmid rescue or the RAPAd systems according to standard protocols.^{63,64} Transgene expression cassettes were constructed in shuttle plasmids via restriction cloning and consisted of either CMV or L7-6³² promoters in combination with the fluorescent reporter proteins mClover3, or mCherry, or mScarlet and chimeric intron, and simian virus polyadenylation signal (SV40polyA) se-

quences. Genomic plasmids for Group B fiber chimeras were constructed from adenovirus Serotype 5 genomic plasmids by excising the shaft and knob sequences of the fiber domain and replacing those with shaft and knob sequences of Serotype 21 (GenBank: AY601633.1, base pairs [bp]: 31,541–32,377), or Serotype 35 (GenBank: AY128640.2, bp: 30,961–31,797), or Serotype 50 (GenBank: AY737798.1, bp: 31,544–32,380). This was achieved by digesting the Ad5 genomic plasmids with Cas9 nuclease (NEB, Ipswich, MA) targeted by single guide RNAs (sgRNAs) spanning the fiber domain with sequences 5'-gggactcttgaacctat-3' upstream and 5'-cttaggtgtatattccaca-3' downstream. The sgRNAs were synthesized using the NEB EnGen sgRNA Synthesis Kit according to the manufacturer's protocol and purified in spin columns (Monarch – NEB, Ipswich, MA). Upon completion, the Cas9 reactions were used as vector DNA in In-Fusion cloning (TakaraBio, San Jose, CA) reactions to insert synthetically manufactured DNA fragments (IDT, Coralville, IA) consisting of fiber domains of Ad21, or Ad35, or Ad50 and terminal 15 bp homology arms. The location and the sequence integrity of the inserts were confirmed by Sanger sequencing. Following co-transfection of genomic and shuttle DNA, all vectors, including the Ad5/GroupB chimeras were serially amplified successfully in the first generation Ad5 producer cell line HEK293. The vectors were then purified based on density by sequential centrifugation in cesium chloride according to standard protocols.⁶⁵

The identities of purified vectors have been confirmed via restriction digestion of PCR fragments amplified using a combination of common primers spanning the fiber domains (upstream: 5'-ttgtatcccccaatgggttcaag, downstream: 5'-gacaggaaacctgtggaatataac). The viral DNA from purified stocks of each vector was extracted in 0.1% SDS at 56°C for 10 min, spin column purified (NucleoSpin – MachereyNagel, Düren, Germany), and PCR amplified via standard Taq polymerase reaction (EconoTaq – Lucigen, Middleton, WI). PCR products were then digested by the restriction enzyme AflIII (NEB, Ipswich, MA) and visualized on 1% agarose gel stained with ethidium bromide. The extracted viral DNA was also used to determine the physical viral titers via absorbance measurement at 260 nm under a UV-Vis spectrophotometer (NanoDrop One – ThermoFisher, Waltham, MA). The titer (viral particles (VP)/mL) was calculated according to standard methods.⁶⁵ The infectious titers (TU/mL) were determined using a droplet digital PCR system (QX200 ddPCR System – Bio-Rad, Hercules, CA) by endpoint amplification of viral DNA extracted from infected HeLa cells via TaqMan assay (ThermoFisher, Waltham, MA). The infectious titers of the vectors were as follows; Ad5 CMV mCherry: 6×10^{10} TU/mL, Ad5/21 CMV mClover3: 1×10^{11} TU/mL, Ad5/35 CMV mClover3: 6×10^{10} TU/mL, Ad5/50 CMV mClover3: 1×10^{11} TU/mL, Ad5/50 CMV mScarlet: 1×10^{11} TU/mL, Ad5/50 L7-6 mScarlet: 3×10^{10} TU/mL.

Stereotactic injections

Mice were anesthetized using a gas anesthesia system (Rothacher, Heitenried, Switzerland) with 5% isoflurane/O₂ mixture and placed on a stereotactic frame (Kopf, Tujunga, CA). Anesthesia was maintained throughout the surgery between 1.5% and 2.5%. Adequate

depth of anesthesia was confirmed by the lack of pedal withdrawal to a toe pinch. Following the scalp application of the local anesthetic (0.5% lidocaine/0.25% bupivacaine mixture - 5 mg/kg), the skull was exposed via an anterior/posterior incision and cerebellum was accessed through craniectomy of a 0.7-mm burr hole. A glass capillary needle coupled with a nanoliter injector (Neurostar, Tübingen, Germany) and loaded with viral vector solution was lowered to coordinates relative to lambda A/P: -2.00 mm, M/L: +1.80 mm, D/V: +2.00 mm for lobular injections targeting the right simple lobule and to A/P: -2.00 mm, M/L: +1.80 mm, D/V: +3.40 mm for DCN injections targeting the right interposed nucleus under guidance of a robot stereotactic system (Neurostar, Tübingen, Germany). One microliter of viral vector solution containing 10^9 VP from each co-mixed vector was infused into the right cerebellar hemisphere at a rate of 100 nL/min and the needle was slowly withdrawn at a speed of 1 mm/min. For the quantification of transduction efficiencies, co-mixed vector titers were matched at 2×10^7 TU each vector. The incision was closed with veterinary tissue adhesive (Med-Vet, Mettawa, IL) and mice were administered Meloxicam SR (2 mg/kg) for postoperative pain management. Following surgical procedures, mice were housed in an ABSL2c facility and daily monitored for adequate recovery for 5 days.

Tissue processing

Mice were anesthetized with isoflurane and euthanized by decapitation. The brain tissue was removed, and right hemispheres were immediately dissected. For the BaseScope assay, dissected tissue was drop fixed in 10% neutral buffered formalin at RT and processed into paraffin blocks via standard embedding protocols. Sagittal sections of 5 μ m were cut using a microtome (HM325 - ThermoFisher, Waltham, MA), mounted on silanized glass slides, and stored at 4°C until further processing. For IF protocols, injected right hemispheres were drop fixed in 4% paraformaldehyde (PFA) at 4°C, cerebellum tissue was further dissected, and serially sectioned into series of 12 using a vibratome (VT1200S - Leica, Nussloch, Germany). Fifty micrometer μ m sagittal cut free-floating sections were preserved at 4°C in phosphate-buffered saline (PBS) containing 0.02% sodium azide until further processing.

RNA *in situ* hybridization: BaseScope assay and brightfield microscopy

Five-micrometer sections were deparaffinized by series of washes in xylene and hydrated in decreasing concentrations of ethanol washes according to standard protocols. BaseScope assay (ACDBio, Newark, CA) was performed following the standard protocol published by the manufacturer using a custom 1ZZ probe designed to target nucleotides 360–410 of human CD46 (GenBank: NM_172351.3) and not to cross detect endogenous mouse transcripts. Chromogenically developed sections (fast red) were counterstained with hematoxylin (VectorLabs, Newark, CA) and coverslipped with Cytoseal XYL (EpreDia, Kalamazoo, MI). Tiled RGB photomicrographs were captured from whole-mount sections under $\times 10$ magnification via brightfield microscopy (DM6 - Leica, Wetzlar, Germany).

IF and confocal imaging

Five-micrometer free-floating sections were treated overnight with 0.01 M sodium citrate (pH = 6.0) at 60°C for antigen retrieval and then permeabilized for 1 h in 0.5% Triton X-/PBS. Sections were blocked in 10% normal goat serum (Jackson ImmunoResearch, West Grove, PA) or with 5% BSA (RPI, Mount Prospect, IL) and incubated in primary antibodies overnight at 4°C. Following biotinylated secondary antibody (VectorLabs, Newark, CA) incubation for 2 h at RT, antigen-antibody complexes were fluorescently labeled with DyLight649 tagged streptavidin (VectorLabs, Newark, CA) during a 1-h incubation at RT. For dual immunolabeling experiments, antigen-primary antibody complexes were visualized with anti-rabbit Alexa 488 and anti-goat Alexa 647 secondary antibodies (Jackson ImmunoResearch, West Grove, PA). Sections were counterstained with DAPI and coverslipped with Aqua-Mount (EpreDia, Kalamazoo, MI). The primary antibodies used were rabbit anti-mouse-Pcp2 C-term (5 μ g/mL, AP6356b - Abcepta, San Diego, CA), goat anti-human-CD46 (0.5 μ g/mL, AF2005 - R&D Systems, Minneapolis, MN), rabbit anti-NeuN (1.5 μ g/mL, 26975-1-AP - Proteintech, Rosemont, IL), rabbit anti-s100 β (2.5 μ g/mL, 15146-1-AP - Proteintech, Rosemont, IL). For the vGlut1 immunofluorescence, a primary antibody directly conjugated to Alexa 647 was used with the secondary antibody omitted (single domain anti-vGlut1-Alexa647, 1:500, N1602-AF647-L - NanoTag, Göttingen, Germany). Coverslipped sections were imaged using a confocal laser scanning microscope (LSM880 - Zeiss, Jena, Germany) under laser lines 405 nm for DAPI, 488 nm for mClover3 vectors and Alexa 488, 561 nm for mCherry and mScarlet vectors, and 633 nm for DyLight649 and Alexa 647 immunolabeled molecular markers. For PC analyses, photomicrographs were acquired under a $\times 20$ objective, whereas a $\times 40$ objective was used for granule cell, mossy fiber, and Bergmann glia images.

Transduced PC number analysis

Fluorescent photomicrographs of serially sectioned hCD46tg cerebellum acquired as tiled whole sections with 2 μ m z-stacks were analyzed with the open-source imaging package Fiji. The transduced PCs were quantified from all sections within a sagittal series of 12, corresponding to an unbiased representation of the right cerebellar hemisphere from its lateral to medial margin. A researcher, blind to the injected viral vectors visually determined labeled PCs from partial images of 350 μ m by 350 μ m generated from tiled whole section scans by a custom cell counter script developed for Fiji. Through the researcher's input, the script recorded the number of transduced PCs by each vector and the number of PCs, on which multiple vector signal co-localizes. The total number of PCs transduced in a section series for each mouse was used for statistical analysis.

Statistical analysis

All statistical analyses were performed using Prism statistical package (GraphPad, Boston, MA). Data were checked for distribution via Shapiro-Wilk normality test. To compare normally distributed group data, unpaired Student's t test with Welch's correction for unequal

standard deviations was performed. A p value of less than 0.05 was considered statistically significant for all analyses and indicated with “*.” $p > 0.05$ was represented with “ns.” Data are summarized as mean (SD).

DATA AND CODE AVAILABILITY

The data in this study will be made available by the corresponding author, S.M.Y., upon reasonable request.

ACKNOWLEDGMENTS

We thank Danielle Yanda and her team for expert technical assistance in colony management and animal care. We thank Iowa Institute of Human Genetics – Genomics Division for sequencing of construct, to University of Iowa Histology Core for their assistance in paraffin tissue processing. We thank University of Iowa Viral Vector Core and their assistance in viral vector production, titer determination, and quality control. The work has been supported by grants from NIDCD (R01 DC014093) and NINDS (R01 NS110742), NCATS R03TR004161-0, CACNA1A Foundation and Orphan Disease Center 2023 Million Dollar Bike Ride pilot grant, and Iowa Distinguished scholar award to S.M.Y. and Iowa Center for Research for Undergraduates research fellowship to A.D. and L.A. Illustrations were created with [Biorender.com](https://biorender.com).

AUTHOR CONTRIBUTIONS

Conceptualization S.M.Y. Methodology E.K. and S.M.Y. Validation E.K. and S.M.Y. Investigation E.K., U.O., A.D., L.P., H.L., P.V.R., and L.A. Formal Analysis E.K., U.O., A.D., L.P., H.L., P.V.R., L.A., and S.M.Y. Resources S.M.Y. Writing-Original Draft E.K. and S.M.Y. Writing-Review & Editing E.K., U.O. and S.M.Y. Visualization E.K., U.O., and S.M.Y. Supervision E.K. and S.M.Y. Project Administration S.M.Y. Funding acquisition S.M.Y.

DECLARATION OF INTERESTS

E.K. and S.M.Y. have a provisional patent filed related to the findings in the manuscript.

REFERENCES

- Bulcha, J.T., Wang, Y., Ma, H., Tai, P.W.L., and Gao, G. (2021). Viral vector platforms within the gene therapy landscape. *Signal Transduct. Targeted Ther.* 6, 53. <https://doi.org/10.1038/s41392-021-00487-6>.
- Dunbar, C.E., High, K.A., Joung, J.K., Kohn, D.B., Ozawa, K., and Sadelain, M. (2018). Gene therapy comes of age. *Science* 359, eaan4672. <https://doi.org/10.1126/science.aan4672>.
- Pupo, A., Fernández, A., Low, S.H., François, A., Suárez-Amarán, L., and Samulski, R.J. (2022). AAV vectors: The Rubik’s cube of human gene therapy. *Mol. Ther.* 30, 3515–3541. <https://doi.org/10.1016/j.jymthe.2022.09.015>.
- Li, C., and Samulski, R.J. (2020). Engineering adeno-associated virus vectors for gene therapy. *Nat. Rev. Genet.* 21, 255–272. <https://doi.org/10.1038/s41576-019-0205-4>.
- Poletti, V., and Mavilio, F. (2021). Designing Lentiviral Vectors for Gene Therapy of Genetic Diseases. *Viruses* 13, 1526. <https://doi.org/10.3390/v13081526>.
- Rothblum-Oviatt, C., Wright, J., Lefton-Greif, M.A., McGrath-Morrow, S.A., Crawford, T.O., and Lederman, H.M. (2016). Ataxia telangiectasia: a review. *Orphanet J. Rare Dis.* 11, 159. <https://doi.org/10.1186/s13023-016-0543-7>.
- Ashizawa, T., Öz, G., and Paulson, H.L. (2018). Spinocerebellar ataxias: prospects and challenges for therapy development. *Nat. Rev. Neurol.* 14, 590–605. <https://doi.org/10.1038/s41582-018-0051-6>.
- Lee, Y., Samaco, R.C., Gatchel, J.R., Thaller, C., Orr, H.T., and Zoghbi, H.Y. (2008). miR-19, miR-101 and miR-130 co-regulate ATXN1 levels to potentially modulate SCA1 pathogenesis. *Nat. Neurosci.* 11, 1137–1139. <https://doi.org/10.1038/nn.2183>.
- Tabrizi, S.J., Estevez-Fraga, C., van Roon-Mom, W.M.C., Flower, M.D., Scahill, R.I., Wild, E.J., Muñoz-Sanjuan, I., Sampaio, C., Rosser, A.E., and Leavitt, B.R. (2022). Potential disease-modifying therapies for Huntington’s disease: lessons learned and future opportunities. *Lancet Neurol.* 21, 645–658. [https://doi.org/10.1016/S1474-4422\(22\)00121-1](https://doi.org/10.1016/S1474-4422(22)00121-1).
- al Yacoub, N., Romanowska, M., Haritonova, N., and Foerster, J. (2007). Optimized production and concentration of lentiviral vectors containing large inserts. *J. Gene Med.* 9, 579–584. <https://doi.org/10.1002/jgm.1052>.
- Kumar, M., Keller, B., Makalou, N., and Sutton, R.E. (2001). Systematic determination of the packaging limit of lentiviral vectors. *Hum. Gene Ther.* 12, 1893–1905. <https://doi.org/10.1089/104303401753153947>.
- Lentz, T.B., Gray, S.J., and Samulski, R.J. (2012). Viral vectors for gene delivery to the central nervous system. *Neurobiol. Dis.* 48, 179–188. <https://doi.org/10.1016/j.nbd.2011.09.014>.
- Watanabe, M., Nishikawaji, Y., Kawakami, H., and Kosai, K.I. (2021). Adenovirus Biology, Recombinant Adenovirus, and Adenovirus Usage in Gene Therapy. *Viruses* 13, 2502. <https://doi.org/10.3390/v13122502>.
- Brunetti-Pierri, N., and Ng, P. (2017). Gene therapy with helper-dependent adenoviral vectors: lessons from studies in large animal models. *Virus Gene.* 53, 684–691. <https://doi.org/10.1007/s11262-017-1471-x>.
- Roelvink, P.W., Lizonova, A., Lee, J.G., Li, Y., Bergelson, J.M., Finberg, R.W., Brough, D.E., Kovcsdi, L., and Wickham, T.J. (1998). The coxsackievirus-adenovirus receptor protein can function as a cellular attachment protein for adenovirus serotypes from subgroups A, C, D, E, and F. *J. Virol.* 72, 7909–7915.
- Jayadev, S., and Bird, T.D. (2013). Hereditary ataxias: overview. *Genet. Med.* 15, 673–683. <https://doi.org/10.1038/gim.2013.28>.
- Storey, E. (2014). Genetic cerebellar ataxias. *Semin. Neurol.* 34, 280–292. <https://doi.org/10.1055/s-0034-1386766>.
- Hoxha, E., Balbo, I., Miniaci, M.C., and Tempia, F. (2018). Purkinje Cell Signaling Deficits in Animal Models of Ataxia. *Front. Synaptic Neurosci.* 10, 6. <https://doi.org/10.3389/fnsyn.2018.00006>.
- Lein, E.S., Hawrylycz, M.J., Ao, N., Ayres, M., Bensinger, A., Bernard, A., Boe, A.F., Boguski, M.S., Brockway, K.S., Byrnes, E.J., et al. (2007). Genome-wide atlas of gene expression in the adult mouse brain. *Nature* 445, 168–176. <https://doi.org/10.1038/nature05453>.
- Hawrylycz, M.J., Lein, E.S., Guillozet-Bongaarts, A.L., Shen, E.H., Ng, L., Miller, J.A., van de Lagemaat, L.N., Smith, K.A., Ebbert, A., Riley, Z.L., et al. (2012). An anatomically comprehensive atlas of the adult human brain transcriptome. *Nature* 489, 391–399. <https://doi.org/10.1038/nature11405>.
- Persson, A., Hober, S., and Uhlén, M. (2006). A human protein atlas based on antibody proteomics. *Curr. Opin. Mol. Therapeut.* 8, 185–190.
- Terashima, T., Miwa, A., Kanegae, Y., Saito, I., and Okado, H. (1997). Retrograde and anterograde labeling of cerebellar afferent projection by the injection of recombinant adenoviral vectors into the mouse cerebellar cortex. *Anat. Embryol.* 196, 363–382. <https://doi.org/10.1007/s004290050105>.
- Hashimoto, M., Aruga, J., Hosoya, Y., Kanegae, Y., Saito, I., and Mikoshiba, K. (1996). A neural cell-type-specific expression system using recombinant adenovirus vectors. *Hum. Gene Ther.* 7, 149–158. <https://doi.org/10.1089/hum.1996.7.2-149>.
- Sato, Y., Shiraiishi, Y., and Furuichi, T. (2004). Cell specificity and efficiency of the Semliki forest virus vector- and adenovirus vector-mediated gene expression in mouse cerebellum. *J. Neurosci. Methods* 137, 111–121. <https://doi.org/10.1016/j.jneumeth.2004.02.014>.
- Baboval, T., Crandall, J.E., Kinnally, E., Chou, D.K., and Smith, F.I. (2000). Restriction of high CD15 expression to a subset of rat cerebellar astroglial cells can be overcome by transduction with adenoviral vectors expressing the rat alpha

- 1,3-fucosyltransferase IV gene. *Glia* 31, 144–154. [https://doi.org/10.1002/1098-1136\(200008\)31:2<144::aid-glia60>3.0.co;2-6](https://doi.org/10.1002/1098-1136(200008)31:2<144::aid-glia60>3.0.co;2-6).
26. Havenga, M.J.E., Lemckert, A.A.C., Ophorst, O.J.A.E., van Meijer, M., Germeeraad, W.T.V., Grimbergen, J., van Den Doel, M.A., Vogels, R., van Deutekom, J., Janson, A.A.M., et al. (2002). Exploiting the natural diversity in adenovirus tropism for therapy and prevention of disease. *J. Virol.* 76, 4612–4620. <https://doi.org/10.1128/jvi.76.9.4612-4620.2002>.
 27. Beatty, M.S., and Curiel, D.T. (2012). Chapter two—Adenovirus strategies for tissue-specific targeting. *Adv. Cancer Res.* 115, 39–67. <https://doi.org/10.1016/B978-0-12-398342-8.00002-1>.
 28. Gaggar, A., Shayakhmetov, D.M., and Lieber, A. (2003). CD46 is a cellular receptor for group B adenoviruses. *Nat. Med.* 9, 1408–1412. <https://doi.org/10.1038/nm952>.
 29. Seya, T., Hirano, A., Matsumoto, M., Nomura, M., and Ueda, S. (1999). Human membrane cofactor protein (MCP, CD46): multiple isoforms and functions. *Int. J. Biochem. Cell Biol.* 31, 1255–1260. [https://doi.org/10.1016/s1357-2725\(99\)00092-8](https://doi.org/10.1016/s1357-2725(99)00092-8).
 30. Johnstone, R.W., Russell, S.M., Loveland, B.E., and McKenzie, I.F. (1993). Polymorphic expression of CD46 protein isoforms due to tissue-specific RNA splicing. *Mol. Immunol.* 30, 1231–1241. [https://doi.org/10.1016/0161-5890\(93\)90038-d](https://doi.org/10.1016/0161-5890(93)90038-d).
 31. Oldstone, M.B., Lewicki, H., Thomas, D., Tishon, A., Dales, S., Patterson, J., Manchester, M., Homann, D., Naniche, D., and Holz, A. (1999). Measles virus infection in a transgenic model: virus-induced immunosuppression and central nervous system disease. *Cell* 98, 629–640. [https://doi.org/10.1016/s0092-8674\(00\)80050-1](https://doi.org/10.1016/s0092-8674(00)80050-1).
 32. Nitta, K., Matsuzaki, Y., Konno, A., and Hirai, H. (2017). Minimal Purkinje Cell-Specific PCP2/L7 Promoter Virally Available for Rodents and Non-human Primates. *Mol. Ther. Methods Clin. Dev.* 6, 159–170. <https://doi.org/10.1016/j.omtm.2017.07.006>.
 33. Li, C., Georgakopoulou, A., Mishra, A., Gil, S., Hawkins, R.D., Yannaki, E., and Lieber, A. (2021). *In vivo* HSPC gene therapy with base editors allows for efficient reactivation of fetal gamma-globin in beta-YAC mice. *Blood Adv.* 5, 1122–1135. <https://doi.org/10.1182/bloodadvances.2020003702>.
 34. Wang, H., Georgakopoulou, A., Li, C., Liu, Z., Gil, S., Bashyam, A., Yannaki, E., Anagnostopoulos, A., Pande, A., Izsvák, Z., et al. (2020). Curative *in vivo* hematopoietic stem cell gene therapy of murine thalassemia using large regulatory elements. *JCI Insight* 5, e139538. <https://doi.org/10.1172/jci.insight.139538>.
 35. Wang, H., Georgakopoulou, A., Psatha, N., Li, C., Capsali, C., Samal, H.B., Anagnostopoulos, A., Ehrhardt, A., Izsvák, Z., Papayannopoulou, T., et al. (2019). *In vivo* hematopoietic stem cell gene therapy ameliorates murine thalassemia intermedia. *J. Clin. Invest.* 129, 598–615. <https://doi.org/10.1172/JCI122836>.
 36. Li, M., Santpere, G., Imamura Kawasawa, Y., Evgrafov, O.V., Gulden, F.O., Pochareddy, S., Sunkin, S.M., Li, Z., Shin, Y., Zhu, Y., et al. (2018). Integrative functional genomic analysis of human brain development and neuropsychiatric risks. *Science* 362, eaat7615. <https://doi.org/10.1126/science.aat7615>.
 37. Zhu, Y., Sousa, A.M.M., Gao, T., Skarica, M., Li, M., Santpere, G., Esteller-Cucala, P., Juan, D., Ferrández-Peral, L., Gulden, F.O., et al. (2018). Spatiotemporal transcriptomic divergence across human and macaque brain development. *Science* 362, eaat8077. <https://doi.org/10.1126/science.aat8077>.
 38. Yamamoto, Y., Nagasato, M., Yoshida, T., and Aoki, K. (2017). Recent advances in genetic modification of adenovirus vectors for cancer treatment. *Cancer Sci.* 108, 831–837. <https://doi.org/10.1111/cas.13228>.
 39. Ridoux, V., Robert, J.J., Zhang, X., Perricaudet, M., Mallet, J., and Le Gal La Salle, G. (1994). Adenoviral vectors as functional retrograde neuronal tracers. *Brain Res.* 648, 171–175. [https://doi.org/10.1016/0006-8993\(94\)91919-4](https://doi.org/10.1016/0006-8993(94)91919-4).
 40. Akli, S., Caillaud, C., Vigne, E., Stratford-Perricaudet, L.D., Poenaru, L., Perricaudet, M., Kahn, A., and Peschanski, M.R. (1993). Transfer of a foreign gene into the brain using adenovirus vectors. *Nat. Genet.* 3, 224–228. <https://doi.org/10.1038/ng0393-224>.
 41. Bajocchi, G., Feldman, S.H., Crystal, R.G., and Mastrangeli, A. (1993). Direct *in vivo* gene transfer to ependymal cells in the central nervous system using recombinant adenovirus vectors. *Nat. Genet.* 3, 229–234. <https://doi.org/10.1038/ng0393-229>.
 42. Nestić, D., Božinović, K., Pehar, I., Wallace, R., Parker, A.L., and Majhen, D. (2021). The Revolving Door of Adenovirus Cell Entry: Not All Pathways Are Equal. *Pharmaceutics* 13, 1585. <https://doi.org/10.3390/pharmaceutics13101585>.
 43. Kügler, S., Meyn, L., Holzmüller, H., Gerhardt, E., Isenmann, S., Schulz, J.B., and Bähr, M. (2001). Neuron-specific expression of therapeutic proteins: evaluation of different cellular promoters in recombinant adenoviral vectors. *Mol. Cell. Neurosci.* 17, 78–96.
 44. Domenger, C., and Grimm, D. (2019). Next-generation AAV vectors-do not judge a virus (only) by its cover. *Hum. Mol. Genet.* 28, R3–R14. <https://doi.org/10.1093/hmg/ddz148>.
 45. Arnberg, N. (2012). Adenovirus receptors: implications for targeting of viral vectors. *Trends Pharmacol. Sci.* 33, 442–448. <https://doi.org/10.1016/j.tips.2012.04.005>.
 46. Wu, H.S., Sugihara, I., and Shinoda, Y. (1999). Projection patterns of single mossy fibers originating from the lateral reticular nucleus in the rat cerebellar cortex and nuclei. *J. Comp. Neurol.* 411, 97–118. [https://doi.org/10.1002/\(sici\)1096-9861\(19990816\)411:1<97::aid-cne8>3.0.co;2-o](https://doi.org/10.1002/(sici)1096-9861(19990816)411:1<97::aid-cne8>3.0.co;2-o).
 47. Barmack, N.H., and Yakhnitsa, V. (2011). Topsy turvy: functions of climbing and mossy fibers in the vestibulo-cerebellum. *Neuroscientist* 17, 221–236. <https://doi.org/10.1177/1073858410380251>.
 48. Nilsson, M., Ljungberg, J., Richter, J., Kiefer, T., Magnusson, M., Lieber, A., Widgren, B., Karlsson, S., and Fan, X. (2004). Development of an adenoviral vector system with adenovirus serotype 35 tropism; efficient transient gene transfer into primary malignant hematopoietic cells. *J. Gene Med.* 6, 631–641. <https://doi.org/10.1002/jgm.543>.
 49. Ni, S., Bernt, K., Gaggar, A., Li, Z.Y., Kiem, H.P., and Lieber, A. (2005). Evaluation of biodistribution and safety of adenovirus vectors containing group B fibers after intravenous injection into baboons. *Hum. Gene Ther.* 16, 664–677. <https://doi.org/10.1089/hum.2005.16.664>.
 50. Cupelli, K., Müller, S., Persson, B.D., Jost, M., Arnberg, N., and Stehle, T. (2010). Structure of adenovirus type 21 knob in complex with CD46 reveals key differences in receptor contacts among species B adenoviruses. *J. Virol.* 84, 3189–3200. <https://doi.org/10.1128/JVI.01964-09>.
 51. Wang, H., Liu, Y., Li, Z., Tuve, S., Stone, D., Kalyushniy, O., Shayakhmetov, D., Verlinde, C.L.M., Stehle, T., McVey, J., et al. (2008). *In vitro* and *in vivo* properties of adenovirus vectors with increased affinity to CD46. *J. Virol.* 82, 10567–10579. <https://doi.org/10.1128/JVI.01308-08>.
 52. Lavoie, A., and Liu, B.H. (2020). Canine Adenovirus 2: A Natural Choice for Brain Circuit Dissection. *Front. Mol. Neurosci.* 13, 9. <https://doi.org/10.3389/fnmol.2020.00009>.
 53. Corjon, S., Gonzalez, G., Henning, P., Grichine, A., Lindholm, L., Boulanger, P., Fender, P., and Hong, S.S. (2011). Cell entry and trafficking of human adenovirus bound to blood factor X is determined by the fiber serotype and not hexon:heparan sulfate interaction. *PLoS One* 6, e18205. <https://doi.org/10.1371/journal.pone.0018205>.
 54. Sakurai, F., Nakamura, S.I., Akitomo, K., Shibata, H., Terao, K., Kawabata, K., Hayakawa, T., and Mizuguchi, H. (2008). Transduction Properties of Adenovirus Serotype 35 Vectors After Intravenous Administration Into Nonhuman Primates. *Mol. Ther.* 16, 726–733. <https://doi.org/10.1038/mt.2008.19>.
 55. Christine, C.W., Richardson, R.M., Van Laar, A.D., Thompson, M.E., Fine, E.M., Khwaja, O.S., Li, C., Liang, G.S., Meier, A., Roberts, E.W., et al. (2022). Safety of AADC Gene Therapy for Moderately Advanced Parkinson Disease: Three-Year Outcomes From the PD-1101 Trial. *Neurology* 98, e40–e50. <https://doi.org/10.1212/WNL.0000000000012952>.
 56. Richardson, R.M., Bankiewicz, K.S., Christine, C.W., Van Laar, A.D., Gross, R.E., Lonser, R., Factor, S.A., Kostyk, S.K., Kells, A.P., Ravina, B., and Larson, P.S. (2020). Data-driven evolution of neurosurgical gene therapy delivery in Parkinson's disease. *J. Neurol. Neurosurg. Psychiatry* 91, 1210–1218. <https://doi.org/10.1136/jnnp-2020-322904>.
 57. Rocco, M.T., Akhter, A.S., Ehrlich, D.J., Scott, G.C., Lungu, C., Munjal, V., Aquino, A., Lonser, R.R., Fiandaca, M.S., Hallett, M., et al. (2023). Long-term safety of MRI-guided administration of AAV2-GDNF and gadoteridol in the putamen of individuals with Parkinson's disease. *Mol. Ther.* 31, 2296. <https://doi.org/10.1016/j.yvmt.2023.04.009>.
 58. Van Laar, A.D., Van Laar, V.S., San Sebastian, W., Merola, A., Elder, J.B., Lonser, R.R., and Bankiewicz, K.S. (2021). An Update on Gene Therapy Approaches for Parkinson's Disease: Restoration of Dopaminergic Function. *J. Parkinsons Dis.* 11, S173–S182. <https://doi.org/10.3233/JPD-212724>.

59. Lonser, R.R., Akhter, A.S., Zabek, M., Elder, J.B., and Bankiewicz, K.S. (2020). Direct convective delivery of adeno-associated virus gene therapy for treatment of neurological disorders. *J. Neurosurg.* *134*, 1751–1763. <https://doi.org/10.3171/2020.4.JNS20701>.
60. Sawada, Y., Kajiwarra, G., Iizuka, A., Takayama, K., Shuvaev, A.N., Koyama, C., and Hirai, H. (2010). High transgene expression by lentiviral vectors causes maldevelopment of Purkinje cells *in vivo*. *Cerebellum* *9*, 291–302. <https://doi.org/10.1007/s12311-010-0161-1>.
61. Kim, Y., Kim, T., Rhee, J.K., Lee, D., Tanaka-Yamamoto, K., and Yamamoto, Y. (2015). Selective transgene expression in cerebellar Purkinje cells and granule cells using adeno-associated viruses together with specific promoters. *Brain Res.* *1620*, 1–16. <https://doi.org/10.1016/j.brainres.2015.05.015>.
62. Zhang, Y., and Bergelson, J.M. (2005). Adenovirus receptors. *J. Virol.* *79*, 12125–12131. <https://doi.org/10.1128/JVI.79.19.12125-12131.2005>.
63. Ng, P., and Graham, F.L. (2002). Construction of first-generation adenoviral vectors. *Methods Mol. Med.* *69*, 389–414.
64. Anderson, R.D., Haskell, R.E., Xia, H., Roessler, B.J., and Davidson, B.L. (2000). A simple method for the rapid generation of recombinant adenovirus vectors. *Gene Ther.* *7*, 1034–1038. <https://doi.org/10.1038/sj.gt.3301197>.